Food Research International 242 (2026) 120006

Contents lists available at ScienceDirect

Food Research International

journal homepage: www.elsevier.com/locate/foodres

Network formation in pea protein–based meat substitutes: effects of pH, oil, and pectin-based microgel particles☆

Désirée Martin, Leon Harnisch, Nico Leister, Ulrike S. van der Schaaf, Felix Ellwanger *

Karlsruhe Institute of Technology (KIT), Institute of Process Engineering in Life Sciences, Chair of Food Process Engineering (LVT), Gotthard-Franz-Straße 3, 76131 Karlsruhe, Germany

ARTICLE INFO

Keywords:
Plant protein structuring
High-moisture extrusion
Alternative proteins
Microgel particles
Emulsions
Protein network

ABSTRACT

As consumer awareness of the environmental and health impacts of excessive meat consumption grows, so does interest in plant-based meat substitutes. High-moisture extrusion of protein isolates is an emerging method for producing anisotropic, meat-like structures. However, sensory differences in texture remain a challenge. This study investigates the formation of protein networks in pea protein isolate (PPI) meat substitutes when the pH is adjusted, in a range of pH 3.3 to 11.1, using either hydrochloric acid or sodium hydroxide, or when canola oil and pectin-based microgel particles (MGP) are added. Network formation was investigated using a closed cavity rheometer, and meat substitutes were produced using a laboratory-scale extruder. Both acidic and alkaline pH adjustments affected the protein network formation. Under acidic conditions, the network is mainly strengthened. Under alkaline conditions, disulfide bond formation was accelerated. The anisotropic, meat-like structure disappeared under acidic conditions, but a slight increase in pH resulted in more pronounced fibrous structures. The addition of oil ($\phi_{oil,max}$ = 3.3 wt%) decelerated the formation of disulfide bonds but did not affect the formation of fibrous structures in the extrudates. MGP did not seem to influence network formation; the structure of the meat substitute remained unchanged. These results demonstrate that the texture of plant-based meat substitutes produced by high-moisture extrusion can be effectively altered by pH modulation and that network formation investigation can indicate structural changes.

1. Introduction

High-moisture extrusion is an established process for the production of meat substitutes. In this process, plant proteins are mixed with liquid formulations, subjected to thermal and mechanical stress, and subsequently pushed through a cooling die (Akdogan, 1999; Arêas, 1992; Cheftel et al., 1992). The fibrous, anisotropic structure is formed in the die adapter and the cooling die, which are intended to imitate the structure of muscle meat (Beniwal et al., 2021; Wittek et al., 2021). Despite the growing availability of meat substitutes, there are still significant sensory differences between meat and its alternatives. Texture is particularly important for meat substitutes because it influences how consumers perceive and accept them (Baig et al., 2025). Consequently, there is a growing interest in methods that allow for the specific modulation of texture.

Several hypotheses have been proposed regarding the structuring of meat substitutes (van der Sman & van der Goot, 2023). However, it should be noted that structuring meat substitutes requires a deformable protein network (McClements, 2024; van der Sman & van der Goot, 2023). Therefore, it is logical to create specific structures by modifying the formation of the protein network. For the modification of protein networks, there are also several methods available. In this paper, we focus on the modulation of the pH and on the addition of oil and pectin-based microgel particles.

A change in pH by adding acids and alkalis, influences the protein-protein interactions, thus influences the network formation directly, and in turn changes the final structure of the protein matrix (Gobes et al., 2025; Li et al., 2026; Nisov et al., 2022). While increased aggregation occurs in the region of the isoelectric point (IEP) due to van-der-Waals forces and hydrophobic effects, a pH shift above the IEP leads to electrostatic repulsion between similarly charged molecules (Totasaus et al., 2002). This reduces the aggregation and thus the cross-linking density of the protein network. These relationships were demonstrated for dry extruded pea protein isolate (IEP ≈ 4.3–4.9) (Muhialdin & Ubbink,

☆ This article is part of a Special issue entitled: 'ALTPROT' published in Food Research International.

* Corresponding author.
E-mail address: felix.ellwanger@kit.edu (F. Ellwanger).

https://doi.org/10.1016/j.foodres.2026.120006
Received 13 April 2026; Received in revised form 24 June 2026; Accepted 10 July 2026
Available online 11 July 2026

2023): with increasing pH (from 5.0 to 9.0), the hardness of the extrudates decreased significantly. It was also observed that soy protein isolate exhibits stronger non-covalent cross-linking closer to the IEP, which is associated with increased complex viscosity (Ellwanger et al., 2024).

In addition to non-covalent bonds, covalent disulfide bonds also influence the formation of the protein network (Schmid et al., 2022). Studies on extruded wheat gluten (IEP = 7.0) show that the pH has a regulating function: under acidic conditions (pH < 5.5), an increased number of free thiol groups was found, which was associated with reduced network formation by disulfide bonds. With increasing pH, disulfide bonds increased and led to increased structural integrity. However, a further increase in pH beyond pH 7 showed no additional effect (Langstraat et al., 2015; Nisov et al., 2022). For extrudates produced with oat protein, it was shown that under alkaline conditions (pH = 7.0–9.0) significantly stronger networks are formed than under neutral or acidic conditions, which was attributed to the increased formation of disulfide bonds (Nieto-Nieto et al., 2015).

The addition of oil and pectin-based microgel particles to the network formation process can be considered as a type of filler addition. This process can be described using the Chen and Dickinson model. The fillers can act as active fillers by being integrated into the protein network via specific interactions and contributing to a strengthening of the network. Conversely, fillers can act as inactive fillers by having no chemical affinity to the formed network. They are surrounded by the network, yet they do not interact with it. Therefore, they can be considered a disturbance to the network, weakening the structure (Chen & Dickinson, 1999).

For the addition of canola oil to pea and soy protein isolate extrudates, it has been stated that canola oil acts as an inactive filler and reduces network strength (Saavedra I. et al., 2023). However, the protein content, which directly influences the protein network, has not been kept constant. Additionally, the rheological properties were measured for structured extrudates, but not for the forming network. The influence of rapeseed oil on the rheological properties and gluten polymerization of gluten doughs used for meat substitutes has been investigated (Opaluwa et al., 2024). It has been shown that oil reduces network strength and polymerization kinetics. However, in this study, the protein content was also not kept constant.

The addition of pectin-based microgel particles to meat substitutes has not yet been investigated. However, MGP have been added to high-protein pea gels ($\phi_{PPI} = 12$ wt%) (Martin et al., 2025). It has been shown that MGP act as inactive fillers, which weaken the resulting protein network.

To investigate the effects of pH modulation, oil addition, and microgel particle addition on the network formation of pea protein-based meat substitutes, temperature sweeps were performed using a closed cavity rheometer. Different pea protein doughs were used, with the addition of hydrochloric acid (HCl), sodium hydroxide (NaOH), canola oil, and pectin-based microgel particles (MGP). To examine how altered network formation impacts the structure of meat substitutes, extrusion trials were conducted on a laboratory-scale extruder under constant extrusion conditions. The resulting extrudates were visually inspected and mechanically characterized by hardness measurements to obtain additional information on the strength and macrostructure of the formed protein network. Additionally, buffer tests investigating the protein-protein interactions were performed for the extrudates and doughs with pH modulation.

A decrease in pH was expected to result in more protein aggregation and stronger networks, as well as less pronounced meat-like structures. An increase in pH was expected to result in greater electrostatic repulsion and a higher number of disulfide bonds. Therefore, no prediction was made regarding the resulting meat-like structure. It was expected that oil and MGP would act as inactive fillers, resulting in weaker protein networks and looser structures that enhance the formation of meat-like structures.

This study should reveal how meat substitutes can be structured by modifying network formation using pH modulation, oil, and MGP as fillers. This would provide a toolbox for creation of anistropic structures. Moreover, investigating how structure formation can be indicated would accelerate formulation engineering and simplify product development.

2. Materials and methods

2.1. Materials

Pea protein isolate (PISANE M9) from yellow peas was obtained from COSUCRA Group Warcoing S.A. (Warcoing, Belgium). According to the manufacturer, the protein content in the PPI was >86%, the fat content <9% while the water content was <7%. Low methylester sugar beet pectin was provided by Herbstreith & Fox GmbH & Co. KG (Neuenbürg, Germany). The pectin exhibited a degree of esterification of 39%, a degree of acetylation of 5%, and a galacturonic acid content of 65%, according to the manufacturer. Canola oil was obtained from Bernhard Schell GmbH (Lichtenau, Germany). The hydrochloric acid utilized in this study was procured from Thermo Fisher Scientific Inc. (Karlsruhe, Germany). The following reagents were obtained from Carl Roth GmbH + Co. (Karlsruhe, Germany): acetone, dithiothreitol (DTT), bovine serum albumin (BSA), calcium chloride dihydrate ($CaCl_2$), urea, potassium chloride (KCl), sodium chloride (NaCl), sodium dihydrogen phosphate dihydrate (NaH_2PO_4), disodium hydrogen phosphate dehydrate (Na_2HPO_4), sodium dodecyl sulfate (SDS), and sodium hydroxide. All chemicals were obtained in analytical grade.

2.2. Protein solubility

The PPI was dried for 72 h at 30 °C and 10 mbar in a Memmert V0101 vacuum drying oven (Memmert GmbH + Co. KG, Schwabach, Germany). To determine protein solubility, 30 mg of the dried PPI was suspended in 30 mL of Milli Q water. The pH was adjusted with NaOH and HCl using an edge HI2020 02 pH meter (HANNAH Instruments, Vöhringen, Germany). The samples were then incubated for 1 h at 25 °C and 200 rpm on an SM 30 circular shaker (Edmund Bühler GmbH, Bodelshausen, Germany). The insoluble components were separated by centrifugation at 4301 RCF (4250 rpm) and 25 °C for 50 min in an Eppendorf 5920 R benchtop centrifuge (Eppendorf SE, Hamburg, Germany). A Quick Start Bradford Protein Assay Reagent (Bio Rad Laboratories GmbH, Munich, Germany) was used for the quantitative determination of protein solubility. The absorbance was then measured at 595 nm using an Evolution 201 UV Vis spectrophotometer (Thermo Fisher Scientific Inc., Waltham, USA). The protein concentration was calculated by calibration with BSA as standard protein. Two sample sets were prepared for each condition and measured three times each. Protein solubility SL was calculated using eq. (1), where c_s corresponds to the concentration of dissolved protein in the supernatant (in BSA equivalent) and c_t corresponds to the theoretical total concentration of the protein used. For c_t, a protein content of 86% was assumed based on the product specification of the raw material supplier.

$$SL = \frac{c_s}{c_t} \bullet 100\% \quad (1)$$

2.3. Determination of the isoelectric point

The isoelectric point was determined by suspending 30 mg of PPI in 30 mL of a 1 mM KCl solution, followed by the same pH adjustment, incubation and separation process as in section 2.2. The zeta potential was measured using a nanoPartica SZ 100 particle analyzer (Horiba Scientific, Kyoto, Japan). Two samples were prepared for each condition, with ten measurements performed on each.

2.4. Preparation of the liquid phases

The addition of acid, alkaline, oil and pectin-based MGP was done via the liquid phase. The liquid phase is needed both for the production of the doughs for the network formation investigation and for the extrusion trials. All formulations were designed so that the total protein content would remain constant in the dough and extrudate at the end, because this content is largely responsible for forming the protein network.

2.4.1. Preparation of microgel particle suspensions

The procedure for preparing the MGP suspensions is based on established methods described in previous studies (Martin et al., 2025; Saavedra Isusi et al., 2021). The MGP were produced via a top-down approach combining ionic gelation and high-pressure homogenization. First, a 2 wt% pectin solution was prepared by dissolving 2 g pectin in 98 g demineralized water at 70 °C under stirring and subsequently cooling the solution to room temperature.

For MGP preparation, the pectin solution was added at a 1:1 volume ratio to a 40 mM $CaCl_2$ solution under dispersion using an ULTRA TURRAX T 25 digital dispersing rod (IKA Werke GmbH & CO. KG, Staufen, Germany) at 13000 rpm. After complete addition, dispersion was continued for 3 min under the same conditions. The resulting 50 wt % MGP suspension was used for further dilution.

The 5 wt% and 10 wt% MGP suspensions were homogenized twice at 621 bar and 25 °C using a Shear Jet HL 60 V2 high-pressure homogenizer (Dyhydromatics LLC, Maynard, Massachusetts, USA). The 3 wt% MGP suspension was prepared by diluting the homogenized 5 wt% suspension with demineralized water. The hydrodynamic diameter of the MGP in all suspensions was 0.81 ± 0.06 µm.

2.4.2. Production of oil-in-water emulsions

A 5 wt% PPI suspension was dispersed with an ULTRA TURRAX T 25 digital dispersing rod (IKA Werke GmbH & CO. KG, Staufen, Germany) at a relative centrifugal acceleration of 1635 RCF (15,000 rpm) for 30 s while 6 wt% of canola oil was added. It was then pre-emulsified for another 30 s under the same conditions. The resulting emulsion was homogenized once at 9 kpsi (621 bar) and 25 °C using a Shear Jet HL 60 V2 high-pressure homogenizer (Dyhydromatics LLC, Maynard, Massachusetts, USA). The 4 wt% and 2 wt% emulsions were prepared by diluting the homogenized 6 wt% emulsions. The mean Sauter diameter of all O/W-emulsions was 0.24 ± 0.01 µm and the volumetric size distribution can be found in Fig. 10 in the supplementary material. The resulting compositions of the O/W-emulsions are given in Table 1.

2.5. Network formation investigation by a temperature sweep

2.5.1. Dough preparation

Doughs with a protein content of 45 wt% and a liquid formulation content of 55 wt% were produced. The water content of the PPI was not considered. The liquid formulations are described in section 2.4. As reference to all liquid formulations, a dough was prepared with demineralized water. Dough samples of 200 g were prepared in a Thermomix TM31 (Vorwerk SE & Co. KG, Wuppertal, Germany). To do this, PPI was first weighed, and the corresponding liquid formulation was added at stirring speed 1 within 10 s. The mixture was then mixed clockwise for 30 s and another 30 s counter-clockwise at stirring speed 5. The doughs were then vacuum-sealed and stored in a refrigerator at 4 °C for 24 h. The compositions of the doughs can be found in Table 2.

Table 1
Composition of oil-in-water-emulsions.

Canola oil / wt%	Pea Protein Isolat / wt%	Water / wt%
6.0	5.0	89.0
4.0	3.3	92.7
2.0	1.7	96.3

Table 2
Composition of the pea protein isolate doughs and extrudates.

PPI / wt%	Water / wt%	MGP / wt%	Canola oil / wt%
45.0	55.0	0.0	0.0
45.0	53.4	1.6	0.0
45.0	52.3	2.7	0.0
45.0	49.5	5.5	0.0
45.0	53.9	0.0	1.1
45.0	52.8	0.0	2.2
45.0	51.7	0.0	3.3

2.5.2. Temperature sweep

The network formation of the protein doughs produced was investigated with a closed cavity rheometer (RPA Flex, TA Instruments Inc., New Castle, DE, USA). Temperature sweeps were performed from 40 °C to 160 °C at a constant heating rate ($dT{\cdot}dt^{-1}$) of 5 $K{\cdot}min^{-1}$. An amplitude γ of 5% and a frequency f of 1 Hz were used, to ensure a stable signal-to-noise ratio within the linear viscoelastic range. For each condition, the measurements were performed three times.

2.6. Extrusion processing for producing meat substitutes

Extrusion tests were performed using a Process 11 Hygienic twin-screw extruder (Thermo Fisher Scientific Inc., Karlsruhe, Germany) equipped with a cooling die. The cooling die had a dimension of H × W × L: 4 × 19 × 125 mm and was tempered to 30°C using a Presto Plus LH 47 cooling circulation thermostat (Julabo GmbH, Seelbach, Germany). The PPI was fed into the first barrel element of the extruder via a DDSR20 twin-screw feeder (Brabender Technology GmbH, Duisburg, Germany). The liquid phase was fed into the third barrel element using a Masterflex L/S peristaltic pump (Cole-Parmer, Vernon Hills, IL, USA). The liquid formulations described in section 2.4 were used for the liquid dosing. The screw had a diameter of 11 mm with a length-to-diameter ratio (L/D) of 40 and the screw configuration comprised two kneading blocks, one behind the liquid feed port and one close to the die adapter. A drawing of the screw configuration can be found in the work of Pernice et al. (Pernice et al., 2025). The screw speed was set to 600 rpm for all experiments. The mass flow of the protein, the mass flow of the liquid formulations, and the temperature profile of the barrel elements are shown in Table 3.

After leaving the cooling die, the extrudates were vacuum-sealed and stored in a freezer at −24 °C. As demonstrated in the study by Nieuwland et al. (Nieuwland et al., 2023), the process of freezing extrudates does not alter their anisotropic, meat-like structure. The resulting compositions of the extrudates with the respective addition of MGP suspensions and O/W-emulsions are shown in Table 2.

2.7. pH-measurements

The pH value was determined using a modified method according to (Meißner, 2016). For this purpose, an extraction mixture was prepared at a ratio of 5:95 (*v*/v) from acetone (5 vol%) and demineralized water (95 vol%). To prepare the samples, 5 g of dough (section 2.5.1) or extrudates (section 2.6) were placed in a mortar, 50 mL of the acetone-water mixture was added, and then ground. The suspension was then transferred to a snap lid jar and dispersed for 30 s with an ULTRA TURRAX T 25 digital dispersing rod (IKA Werke GmbH & CO. KG, Staufen, Germany) at 7 RCF (1000 rpm). The pH value of the

Table 3
Mass flow of the protein powder and the liquid phase, as well as the temperature profile of the barrel elements.

$\dot{m}_P$ / $kg{\cdot}h^{-1}$	$\dot{m}_L$ / $kg{\cdot}h^{-1}$	T_2 / °C	T_3 / °C	T_4 / °C	T_5 / °C	T_6 / °C	T_7 / °C	T_8 / °C	$T_{adapter}$ / °C
0.23	0.28	25	50	90	100	140	140	140	30

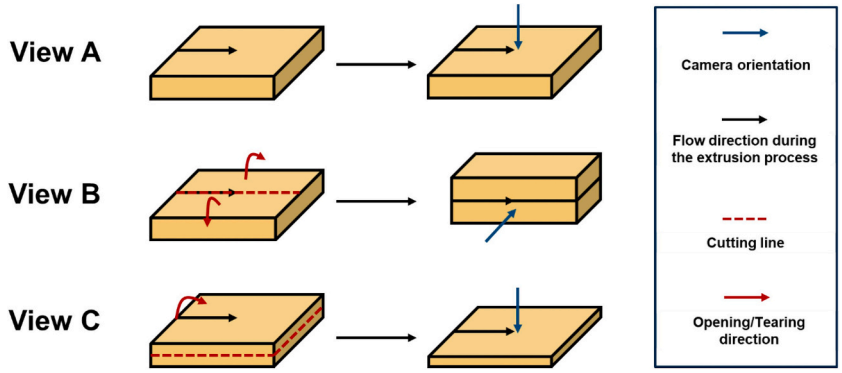

Fig. 1. Preparation of the extrudates for visualisation of the macrostructure. (A) View of the unprepared extrudate from above. (B) Longitudinal section along the flow direction. (C) Torn sample after lateral incision.

suspensions was determined using an edge HI2020 02 pH meter (HANNAH Instruments, Vöhringen, Germany). Three suspensions were prepared and measured once for each condition.

2.8. Sample visualisation

The macrostructure was visualized using three approaches, as shown in Fig. 1: (A), the extrudate was photographed from above. (B), the extrudate was cut open along the center of the flow direction and unfolded to reveal the internal structure in a longitudinal section. (C), the extrudate was cut along the narrow side surfaces and then torn open in the flow direction to assess the meat-like structure inside.

2.9. Texture profile analysis (TPA)

A mechanical texture analysis of the extrudates was performed using TPA on a HAAKE MARS 60 rheometer (Thermo Scientific GmbH, Karlsruhe, Germany). A plate-plate system with a diameter of 35 mm was used. For sample preparation, cylindrical samples with a diameter of 6 mm were punched out from the middle of the extrudates. The samples were compressed twice at 22 °C to 50% of their original height. The test speed was 0.25 mm·s^{-1}, with a defined waiting time of 2 s between the two compressions. Three samples were prepared for each extrudate and measured once. The peak maximum force at first compression was taken as the hardness.

2.10. Degree of aggregation

The protein doughs produced in section 2.5 and the extrudates from section 2.6 were dried for 24 h at 50 °C in a UT 60 drying oven (Heraeus Holding GmbH, Hanau, Germany). These were then milled using a KOENIC KCH 2021 mill (Imtron GmbH, Ingolstadt, Germany) and sieved (280 µm mesh) to achieve a particle size of <280 µm. The resulting powders were dried for 72 h at 30 °C and 10 mbar in a Memmert VO101 vacuum drying oven (Memmert GmbH + Co. KG, Schwabach, Germany). To investigate protein-protein interactions, the dried and ground samples were suspended in three different phosphate buffer systems. The three buffers contained 0.132 M Na_2HPO_4 and 0.068 M NaH_2PO_4, which were used to buffer the pH of 6.9. Buffer 1 (PBS 1) was a phosphate buffer to which 0.05 M NaCl was added and was used to extract proteins in their initial state. Buffer 2 (PBS 2) contained 0.0173 M SDS, 8 M urea, and 0.05 M NaCl. These chemicals enabled the dissociation or inhibition of electrostatic interactions, hydrogen bonds, and hydrophobic interactions. Buffer 3 (PBS 3) was based on the composition of PBS 2 and additionally contained 0.01 M DTT to cleave disulfide bonds. For analysis, 20 mg of each sample was suspended in 20 mL of the corresponding buffer. The samples were then incubated for 2 h at 25 °C and 200 rpm on an SM 30 circular shaker (Edmund Bühler GmbH, Bodelshausen, Germany). After incubation, insoluble protein fractions were separated by centrifugation at 4301 RCF (4250 rpm) and 25 °C for 50 min in a 5920 R benchtop centrifuge (Eppendorf SE, Hamburg, Germany). A Pierce 660 nm Protein Assay Reagent (Thermo Fisher Scientific Inc., Waltham, USA) was used for the quantitative determination of the dissolved proteins. To ensure compatibility with ionic detergents, this was supplemented with the corresponding compatibility reagent for ionic detergents for the Pierce 660 nm Protein Assay Reagent (ThermoFisher Scientific Inc., Waltham, USA). 10 µL of the supernatant was pipetted into a microtiter plate and mixed with 150 µL of the protein assay. The absorbance was then measured at 660 nm in an Infinite M200 PRO microplate reader (Tecan Trading AG, Männedorf, Switzerland). The protein solubility SL was determined according to eq. (1) in section 2.2. The protein concentration was calculated by calibration with BSA as standard protein for each buffer. For the quantitative evaluation of protein-protein interactions, the differences in protein solubility between the different buffer systems were used as a measure of the respective degree of aggregation. A modified method according to Gräfenhahn was used (Gräfenhahn & Beyrer, 2025). The degree of aggregation due to non-covalent bonds $D_{A,nC-B}$ was determined according to eq. (2) as the difference in protein solubility between PBS 2 and PBS 1. The degree of aggregation due to covalent disulfide bonds $D_{A,S-B}$ was determined according to eq. (3) as the difference between PBS 3 and PBS 2.

$$D_{A,nC-B} = SL_{PBS\,2} - SL_{PBS\,1} \quad |\text{Aggregation through non} - \text{covalent bonds} \tag{2}$$

$$D_{A,S-B} = SL_{PBS\,3} - SL_{PBS\,2} \quad |\text{Aggregation through covalent disulfide bonds} \tag{3}$$

2.11. Statistical analysis

The statistical analysis of the data was conducted using one-way analysis of variance (ANOVA), with a Tukey test employed as a post hoc analysis. Statistical significance was considered as a threshold of $p \leq 0.05$. The statistical analysis and calculation of mean values and standard deviations were conducted using Origin Pro 2023 software (Origin Lab Corp., Northampton, Massachusetts, USA).

3. Results and discussion

3.1. Solubility and surface charge of pea protein isolate

The functional properties of proteins, such as solubility, vary depending on the commercially available protein source and the processing history (Ebert et al., 2020; Schumacher et al., 2025). Therefore, the solubility of the PPI was determined as a function of pH. Since solubility also depends on the surface charge of proteins, zeta potential

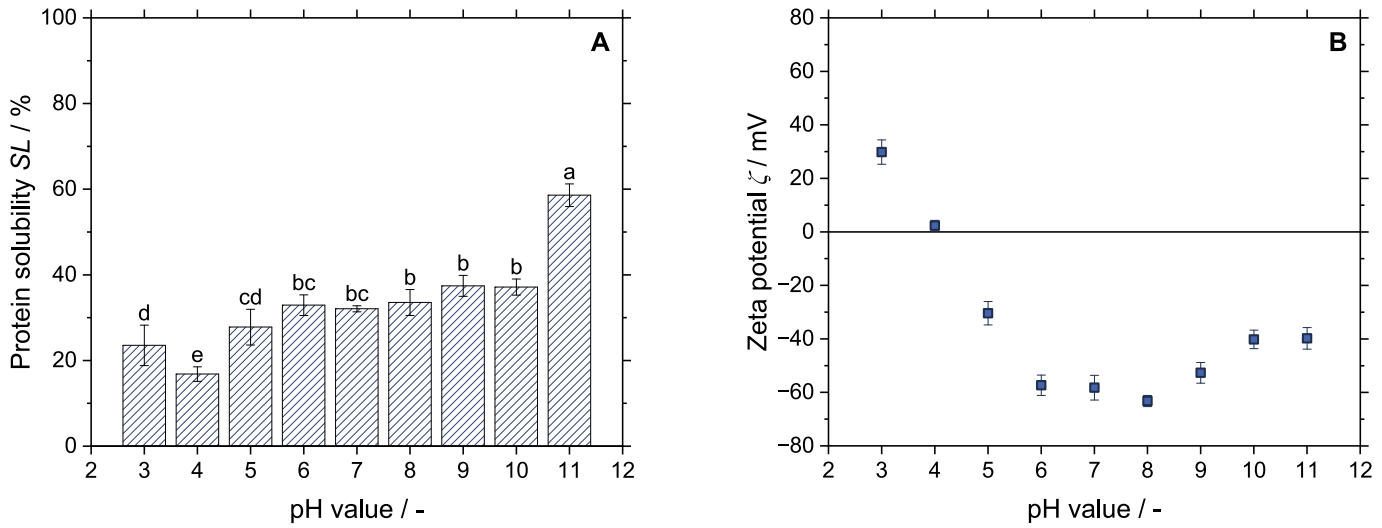

Fig. 2. Protein solubility SL (A) and zeta potential ζ (B) of the pea protein isolate are used as a function of pH value.

measurements were performed in the same pH range (Grossmann & McClements, 2023). Fig. 2 shows the protein solubility SL (A) and the zeta potential ζ (B) of the PPI as a function of pH.

Protein solubility (Fig. 2 A) exhibits a characteristic dependence on the pH. At a pH of 4, solubility is at its lowest. As the pH value deviates from 4, solubility increases and reaches a maximum at pH 11.

This behavior is consistent with the zeta potential results (Fig. 2 B), which reflect the surface charge and electrostatic interactions of the proteins. At pH 4, the zeta potential is close to zero (2.35 ± 1.97 mV) corresponding to the IEP of the PPI (Grossmann & McClements, 2023). At the IEP, electrostatic repulsion between protein molecules is minimized, allowing hydrophobic and van-der-Waals interactions to dominate and promoting aggregation, which results in low solubility (Tokmakov et al., 2021).

At pH values below and above the IEP, the magnitude of the zeta potential increases, indicating greater net positive or negative surface charge. The resulting electrostatic repulsion between similarly charged protein molecules inhibits aggregation and enhances solubility (Grossmann & McClements, 2023; Kishore et al., 2012). The particular high solubility at pH 11 may additionally be attributed to partial protein unfolding under alkaline conditions, which further promotes protein-water interactions (Lagrain et al., 2010).

3.2. Influence of pH, oil incorporation, and pectin-based microgel particles on protein network formation

Temperature sweeps were performed to obtain information on the network formation and the resulting network strength of the PPI doughs under extrusion-relevant temperatures. Fig. 3 shows the magnitude of the complex shear modulus ($|G^*|$) as a function of temperature (T) for the doughs prepared with different liquid formulations.

Fig. 3 A shows the influence of acid addition, Fig. 3 B shows the influence of alkali addition, Fig. 3 C the influence of oil incorporation, and Fig. 3 D shows the influence of pectin-based MGP. In all figures, the addition of pure water to the PPI (gray dots) is given as a reference. For pure water addition, $|G^*|$ decreases steadily over the investigated temperature range. This decrease can be attributed to both increased molecular mobility of the protein molecules and thermally induced degradation reactions, which are expected for PPI from temperatures of around 140 °C (Emin et al., 2017; Liu et al., 2025; Opaluwa et al., 2024; Wittek et al., 2020).

The addition of acid leads to a vertical shift to higher values of $|G^*|$. For example, at 100 °C, it increases from 25 kPa at pH 7.4 to 54 kPa at pH 5.3, 118 kPa at pH 4.4, and 149 kPa at pH 3.4. The increase in $|G^*|$ at a pH of 5.3 and 4.4 can be correlated with the approximation to the IEP (pH 4), which results in reduced electrostatic repulsion between the proteins and favors aggregation (see Fig. 2 B) (Grossmann & McClements, 2023). These results are consistent with results from soy protein isolate doughs, which formed more non-covalent bonds with a pH shift towards IEP (Ellwanger et al., 2024).

Interestingly, the dough with a pH of 3.4 shows the highest value of $|G^*|$, even though the pH is below the IEP. Below the IEP, increased electrostatic repulsion is expected, which reduces the formation of intermolecular interactions and thus network strength (Grossmann & McClements, 2023). It is assumed that acid-induced denaturation exposes hydrophobic groups and enables additional intermolecular interactions, thereby leading to a strengthening of the protein network (Foegeding et al., 1995; Muzammil et al., 1999).

The addition of alkali, as shown in Fig. 3 B results in curves of $|G^*|$ that differ from the pure water curve mainly between 60 °C and 120 °C for pH 8.7 and 9.9, and in a pronounced vertical shift at pH 11.1. At pH 8.7 and 9.9, the curves show an altered temperature dependence, with a smaller initial decrease of $|G^*|$ and a faster final decrease of $|G^*|$ until the curves coincide again at 120 °C. This altered temperature dependency at pH 8.7 and 9.9 could be correlated with changes in disulfide bond formation. Disulfide bond formation is expected to be favored under alkaline conditions and more disulfide bonds lead to a stronger network (Muhialdin & Ubbink, 2023; Pietsch et al., 2017; Scheraga et al., 1962). However, at temperatures above 120 °C, the curves converge again, indicating that disulfide bond formation is complete. Thus, at pH 8.7 and 9.9, disulfide bond formation is expected to have a faster kinetic than when only water is added, which could be explained by enhancing the reactivity of thiol groups under alkaline conditions (Muhialdin & Ubbink, 2023). The PPI dough with a pH value of 11.1 shows a similar temperature-dependent $|G^*|$ compared to the dough with a pH value of 9.9. However, $|G^*|$ is shifted vertically to higher $|G^*|$ over the entire temperature range. Under alkaline conditions, it has been shown that disulfide bonds can also be formed at room temperature (Monahan et al., 1995). This cross-linking can contribute to structure formation even before thermally induced processes start. In addition, the protein structure can unfold under strongly alkaline conditions, making reactive groups accessible and enabling intermolecular interactions (Muzammil et al., 1999).

With increasing oil content, as shown in Fig. 3 C, $|G^*|$ decreases faster than in the pure water sample in the temperature range between 60 °C and 120 °C. As the curves converge at 120 °C, these results can be correlated with disulfide bond formation. Although alkaline conditions seem to favor disulfide bond formation, the addition of oil appears to

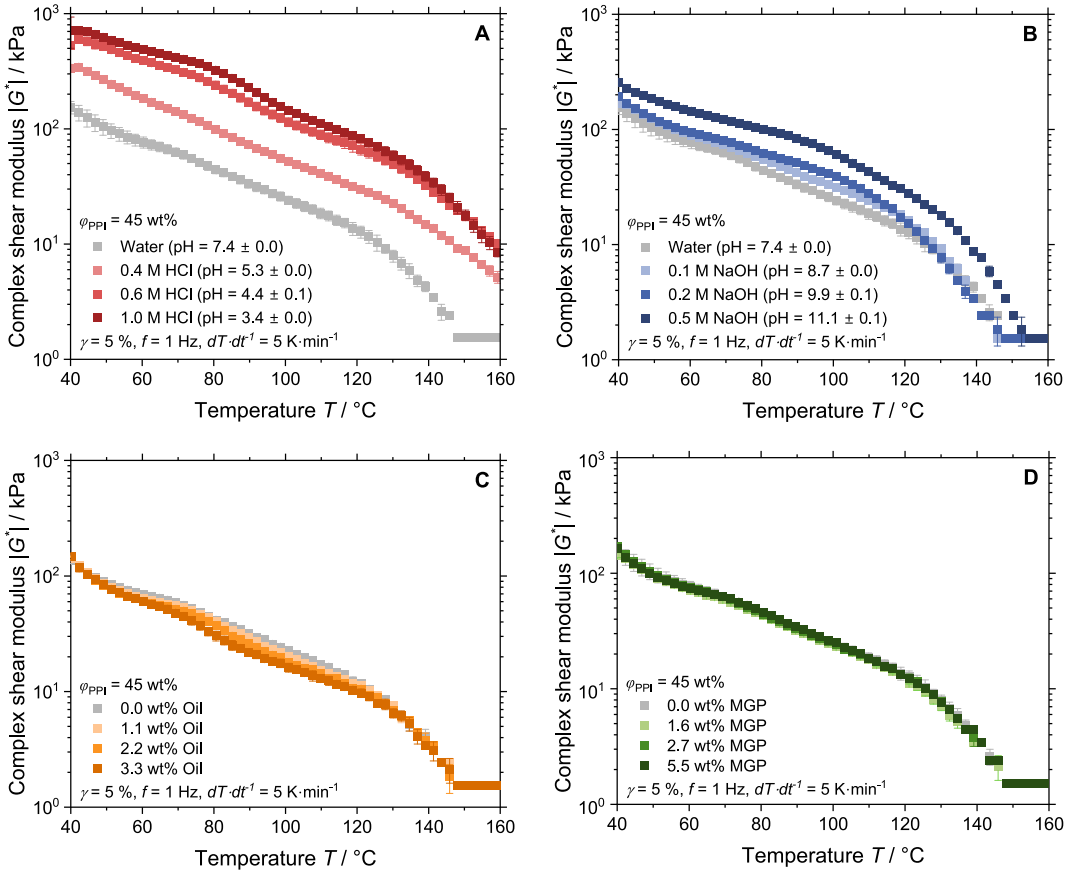

Fig. 3. Change in complex shear modulus |G*| as a function of temperature T for doughs made from pea protein isolate with added hydrochloric acid (A), added sodium hydroxide (B), different oil concentrations (C), and different MGP concentrations (D).

decelerate disulfide bond formation.

No significant differences were found for $|G^*|$ with the addition of different MGP concentrations. Accordingly, the formation and strength of the protein network are not influenced by the addition of MGP, indicating that MGP acts neither as an active nor an inactive filler. Furthermore, no thermo-reversible behavior of the MGP was observed, as no differences in rheological behavior between the reference and MGP-containing samples were detected over the entire temperature range, including at the initial temperature of the temperature sweeps.

Based on the network formation results, the addition of acids under all investigated conditions may promote the formation of denser and stronger protein networks. Accordingly, these networks could exhibit increased mechanical stability during extrusion, which may potentially result in less structured extrudates.

For alkaline conditions (excluding pH 11.1) and the addition of oil, it is not possible to make a clear prediction. While the curves below 60 °C and above 120 °C largely correspond to the reference curves, typical extrusion conditions are found mainly in the intermediate temperature range. Due to the unknown time-temperature profiles in the extruder and the associated reaction kinetics, especially with regard to disulfide bond formation and its influence on structuring, the resulting network behavior cannot be clearly predicted. At pH 11.1, similar to the addition of acids, the results suggest the formation of a stronger protein network. Accordingly, the network may be more difficult to deform during extrusion, potentially resulting in reduced structure formation. For the addition of pectin-based MGP, no significant changes in the extrudate structure are expected.

3.3. Influence of acid, alkali, oil, and pectin-based microgel particle addition on the structure and mechanical properties of meat substitutes

To investigate how different network formation behaviors under extrusion conditions influence structure formation, the described formulations were extruded under constant extrusion parameters. The typical control parameters, temperature at the die adapter, pressure at the die adapter and torque of the motor varied only slightly (128–132 °C, 3–10 bar, 6–8%), and did not indicate any systematic changes in thermomechanical processing conditions.

The macrostructure of the extrudates was evaluated by a visual analysis. Fig. 4 shows macroscopic images of the extrudates with pH reduction with hydrochloric acid.

The extrudate, exhibiting a native pH value of 7.4, has a yellowish color and a smooth surface (view A). In the cross-sectional images (view B), fibrous, anisotropic structures can be identified, which are aligned along the laminar flow profile in the extruder (view C). Upon the addition of acid, the extrudates exhibited a lighter coloration on the outer surface (view A). The cross-sectional images (views B and C) show less pronounced anisotropic, fibrous structures. This observation is consistent with previous studies, according to which meat-like structures in soy protein isolate were less pronounced at a pH value of 5.8 and were no longer detectable when the pH was further reduced (Ellwanger et al., 2024). The temperature sweep in the closed cavity rheometer showed that a reduction in pH leads to a strengthening of the protein network (Chapter 3.2.). This may suggest that under extrusion conditions, the deformation and shear forces acting in the cooling die and die

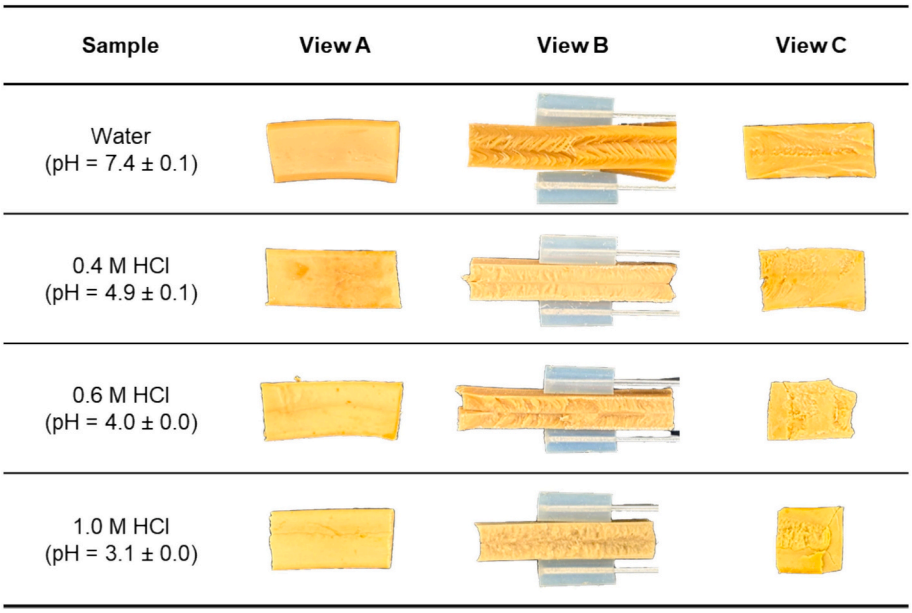

Fig. 4. Macroscopic images of the extrudates at different pH values, adjusted by adding defined concentrations of hydrochloric acid. The samples are shown in three views: (A) view from above, (B) longitudinal section along the flow direction, and (C) sample torn open along the flow direction after lateral incision.

adapter of the extruder were insufficient to sufficiently deform the stronger protein network, preventing the formation of pronounced macroscopic structures.

Fig. 5 shows macroscopic images of the extrudates depending on the pH increased with sodium hydroxide.

The addition of 0.1 M NaOH results in an extrudate with a pH value of 8.8 that is indistinguishable in outer appearance from the extrudate with a native pH value of 7.4 (view A). However, the cross-sectional images show a more pronounced formation of anisotropic, meat-like structures (view B), which are aligned along the laminar flow profile (view C). The temperature sweeps (Chapter 3.2) showed a change in disulfide bond formation between 60 °C and 120 °C. Assuming the same time-temperature profile under constant extrusion conditions, this suggests that the formation of a larger number of disulfide bonds could lead to a more pronounced anisotropic structure. The extrudate with a pH value of 10.0 has a darker color (view A). In the cross-sectional images, anisotropic, meat-like structures are visible (view B), but not oriented along the laminar flow profile (view C). The temperature sweeps in the CCR (Chapter 3.2) showed that disulfide bond formation was altered. Thus, this change in structure could be attributed either to insufficient shear and elongational forces resulting from a stronger protein network, or to a change in the structure formation mechanism caused by altered cross-linking behavior.

The extrudate with a pH value of 10.9 shows a noticeably dark color (view A). One potential explanation for the color change is the alkaline-induced hydrolysis of protein chains, which releases aromatic amino acids (Csapá et al., 1997; Schwass & Finley, 1984). It is assumed that tyrosine and tryptophan, in particular, could contribute to the formation

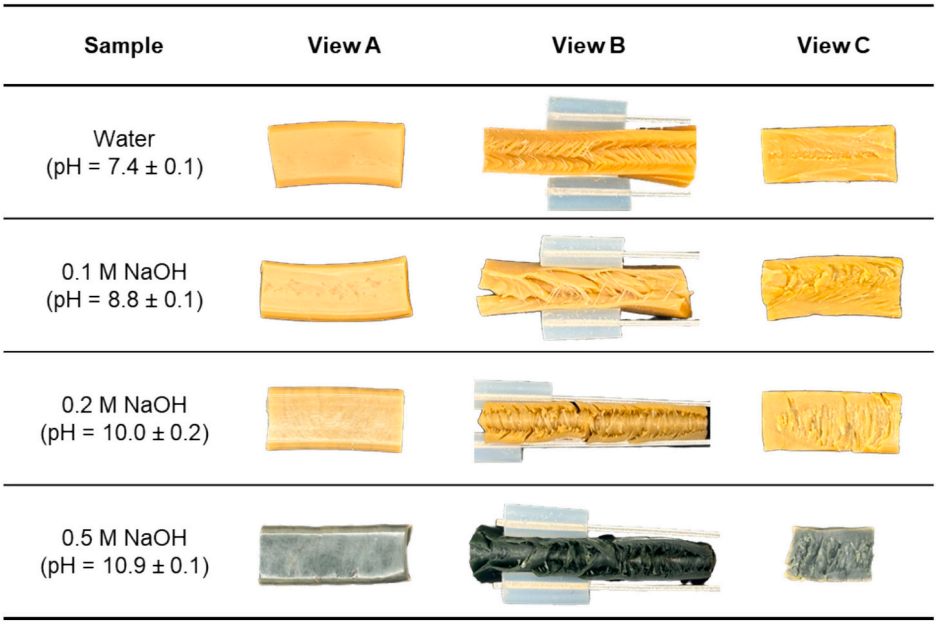

Fig. 5. Macroscopic images of the extrudates at different pH values, adjusted by adding defined concentrations of sodium hydroxide. The samples are shown in three views: (A) view from above, (B) longitudinal section along the flow direction, and (C) sample torn open along the flow direction after lateral incision.

of colored reaction products under strongly alkaline conditions. The observations described for the extrudate with a pH value of 10.0 can also be observed here, but in an even more pronounced form. Anisotropic structures are visible (view B), but there is no orientation along the flow profile (view C). The temperature sweeps in the CCR (Chapter 3.2) showed increased network strength across the entire temperature range in this context.

Hardness tests were additionally performed to investigate the mechanical properties of the structured extrudates. Fig. 6 shows the dependence of hardness on pH. As expected from the network formation experiments, decreasing the pH resulted in harder extrudates, which is assumed to be caused by increased protein–protein interactions closer to the isoelectric point.

Interestingly, the hardness of the structured extrudates produced under alkaline conditions differed only slightly from the sample at pH 7.4, with a significant decrease in hardness observed only at pH 8.8. Overall, this decrease was small compared to the pronounced increase in hardness observed at lower pH values. Based on the network formation behavior under alkaline conditions, harder extrudates might have been expected, as additional disulfide bond formation under constant extrusion conditions may have resulted in stronger protein networks. Furthermore, at pH 10.9, the network formation experiments showed a shift towards higher $|G^*|$ values, which could suggest increased network strength under these conditions. However, this was not reflected in the hardness of the resulting structured extrudates. One potential explanation for these findings could be that the hardness measurements were influenced by differences in macroscopic structure formation.

The results suggest that adjusting the pH value can be used to specifically modify protein network formation and, consequently, the formation of anisotropic, meat-like structures, as has also been demonstrated for pH-modified soy protein concentrates used as meat substitutes (Kuijpers et al., 2025). It appears that there is a pH value at which structuring meat-like products is favored, reflecting a balance between electrostatic interactions and aggregation effects, as additional bonding mechanisms such as disulfide bonds or acid-induced interactions may influence anisotropic structure formation. This is further investigated in the chapter 3.4 by analysing protein–protein interactions in the extruded samples.

Fig. 7 shows macroscopic images of the extrudates produced with different canola oil contents.

The outer appearance (view A) shows a comparable appearance to all extrudates without any notable differences. In the cross-sectional images, meat-like, anisotropic structures are visible in all formulations (view B), which are aligned along the flow profile in the extruder (view C). Visually, there are no discernible differences in the structural properties of these materials when comparing the extrudates.

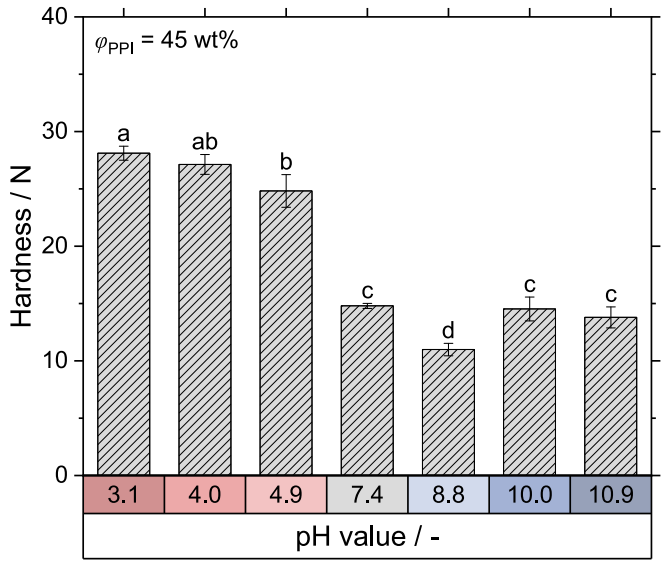

Fig. 6. Mechanical texture parameter of texture profile analysis: hardness as a function of pH value.

The hardness investigation of extrudates with oil addition is shown in the supplementary material in Fig. 11 A. In general, oil addition led to a small decrease in hardness. However, with increasing oil content, the hardness increased again. A potential explanation could be that, at higher oil contents, less water was available for incorporation into the protein network. Nevertheless, these observations suggest that the structure-forming effect was maintained even at higher oil contents. Thus, potentially reduced disulfide bond formation did not appear to negatively affect the formation of fibrous structures. Additionally, neither the macroscopic structure of the extrudates nor the observed hardness changes indicate that the oil acted as an active filler within the protein network. Reasons for these findings, in contrast to literature, could be due to the constant protein content, the low oil concentration added or its incorporation as an emulsion.

Fig. 8 shows macroscopic images of the extrudates produced with different MGP contents.

In the external view (view A), all extrudates exhibit a comparable appearance, with no discernible differences. In the cross-sectional images, meat-like, anisotropic structures can be identified in all formulations (view B), which are aligned along the laminar flow profile in the cooling die (view C). No differences in the characteristics of these structures are apparent between the extrudates. The hardness of the extrudates was decreasing slightly with MGP addition, as can be seen in the supplementary material in Fig. 11 B. Accordingly, the MGP did not appear to act as active fillers within the protein network, and the formation of anisotropic, fibrous structures was not influenced, as expected from the results of the closed cavity rheometer. This may be due to structural transformation of the MGP under thermomechanical stresses during extrusion, potentially leading to altered pectin integration and water release. However, as MGP consist predominantly of water, the overall water content across samples remains largely unchanged and the low pectin concentration likely limits any impact on structuring. In contrast to previous observations in yogurt-type PPI gels at lower protein concentrations (Martin et al., 2025), where MGP showed a structuring effect, this effect could not be reproduced at the higher protein levels investigated here. This suggests that either higher MGP concentrations or more stable particles that withstand processing conditions may be required.

3.4. Degree of aggregation

The extrudates with the addition of acid and alkali have shown macroscopic changes in their structural appearance, and it has been argued that the formation of non-covalent, and covalent disulfide bonds could be the cause. Therefore, the protein-protein interactions of these extrudates and the untreated protein doughs have been investigated. Fig. 9 presents the degree of aggregation (D_A) in the untreated doughs (A) and extrudates (B) as a function of pH value.

The analysis of the doughs (Fig. 9 A) showed that, at a native pH value of 7.4, the protein aggregates are predominantly stabilized by non-covalent bonds. As expected, a shift in pH towards the IEP leads to an increase in non-covalent bonds, as the electrostatic repulsion between protein molecules decreases, favoring van der Waals forces and hydrophobic effects (Grossmann & McClements, 2023; Totosaus et al., 2002). For pH-reduced doughs, the contribution of disulfide bonds to the stabilization of the aggregates is reduced. In the alkaline doughs, aggregation via non-covalent bonds is reduced from a pH value of 9.9 and 11.1. Additionally, at a pH value of 11.1 an increase in disulfide bonds can be observed.

The extrudates (Fig. 9 B) show less aggregation via non-covalent bonds and increased stabilization via disulfide bonds compared to the pH value for corresponding doughs, except for the extrudate at pH value

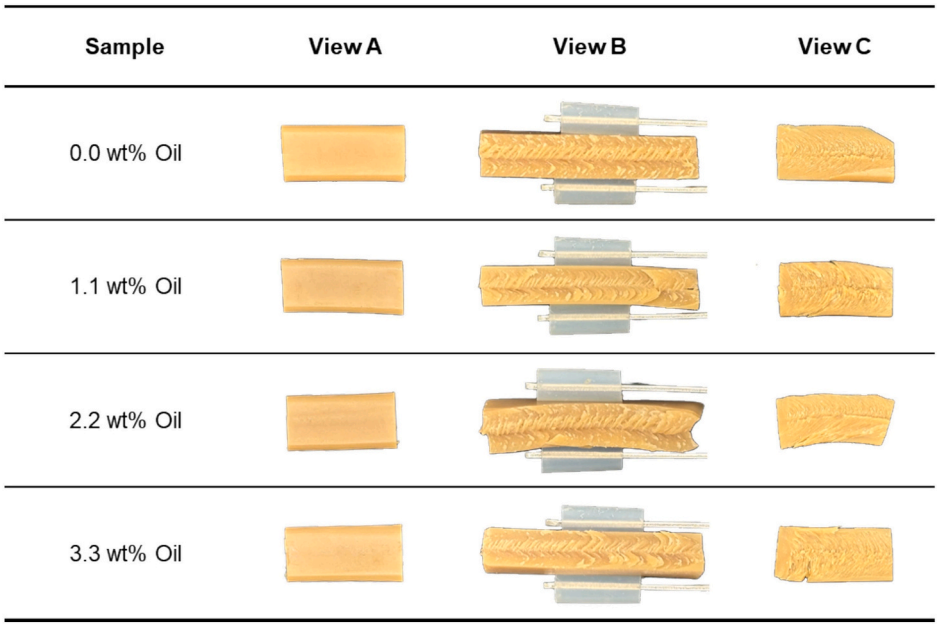

Fig. 7. Macroscopic images of the extrudates with different oil contents. The samples are shown in three views: (A) top view, (B) longitudinal section along the flow direction, and (C) sample torn open along the flow direction.

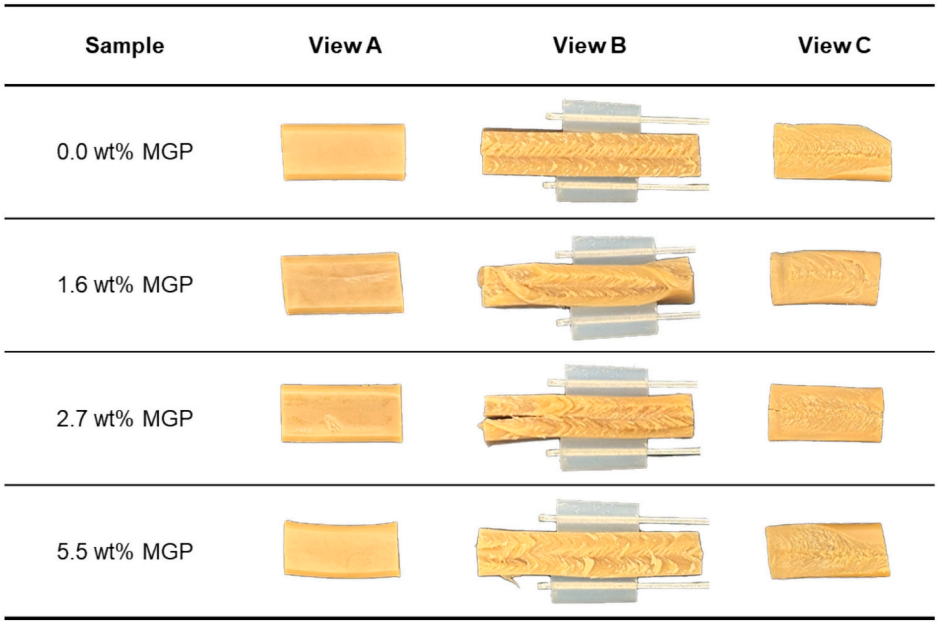

Fig. 8. Macroscopic images of the extrudates with different microgel particle contents. The samples are shown in three views: (A) top view, (B) longitudinal section along the flow direction, and (C) sample torn open along the flow direction.

of 10.9. The thermal and mechanical treatment that takes place during extrusion can break heat-sensitive, non-covalent bonds and lead to the unfolding of protein chains and exposure of functional groups (Beniwal et al., 2021; Harper, 2019). This can result in the formation of new disulfide bonds, which contribute to the stabilization and cross-linking of the protein aggregates (Arêas, 1992). As with doughs, a shift in pH towards the IEP leads to an increase in non-covalent bonds, while disulfide bonds systematically decrease. In the alkaline extrudates, a decrease in non-covalent bonds can be observed. At the same time, the stabilization of the aggregates via disulfide bonds increases, except a pH value of 10.9. Interestingly, at a pH value of 10.9, a significant decrease in both non-covalent and disulfide bonds can be observed.

The findings of the network formation of the doughs (Chapter 3.2) as well as the visual and mechanical examinations of the extrudates (Chapter 3.3) can be supported by the results of the protein-protein interactions. The increased network strength of the acidic doughs observed in the temperature sweeps can be attributed to enhanced non-covalent aggregation when approaching the IEP. Under constant extrusion conditions, this stronger protein network is less deformable, resulting in less pronounced macroscopic structure and the formation of a harder extrudate (Ellwanger et al., 2024).

The altered disulfide bond formation found for the alkaline doughs in the screening tests between 60 °C and 120 °C can be found again in an increase in stabilization via disulfide bonds for the extrudates at a pH

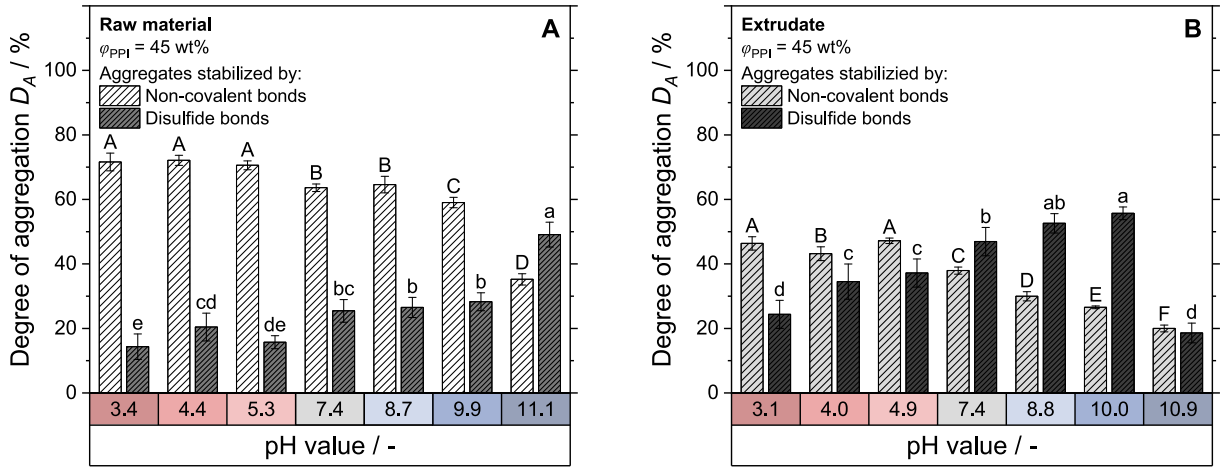

Fig. 9. Degree of aggregation D_A of protein aggregates in the raw material (A) and extrudate (B) as a function of pH value.

value of 8.8 and a pH value of 10.0. If constant processing conditions yield an equivalent time temperature profile across samples, the observed increase in disulfide bonds can be attributed solely to an accelerated disulfide bond formation. The increased network strength of the alkaline dough with a pH value of 11.1 in the temperature sweeps is expected to result from the formation of disulfide bonds at room temperature. Interestingly, the degree of aggregation decreases after extrusion at a pH of 10.9, which could indicate that the protein forms covalent bonds that are not stabilized via disulfide bonds. A possible explanation could be the formation of lysinoalanine cross-links under alkaline and thermally induced conditions (Koyama et al., 2020; Wu et al., 2025). Since the extraction approach used in this study only differentiates between non-covalent interactions and disulfide-bond-stabilized aggregates, the formation of covalent lysinoalanine bonds could not be determined.

Overall, the results indicate that a lower extent of non-covalent interactions combined with a higher degree of disulfide bonding could be beneficial for structuring, although the sample at pH 10 represents an exception as it shows high disulfide bonding but comparatively weaker structuring. This relationship should be further validated in other protein systems such as soy or wheat gluten.

4. Conclusions

This study aimed to investigate the network formation and the resulting influence on structure formation in pea protein-based meat substitutes when the pH is modified or oil or microgel particles are added.

A shift in pH towards the IEP (pH ≈ 4) resulted in less pronounced anisotropic structures and harder extrudates, which could be attributed to increased aggregation via non-covalent bonds. Temperature sweeps in the CCR indicated stronger protein networks under extrusion-relevant temperatures, which may have limited deformation and texturing during extrusion.

In the alkaline range, aggregation via disulfide bonds increased, while aggregation via non-covalent bonds decreased. At pH 8.7, enhanced formation of anisotropic structures was observed, whereas further increasing the pH resulted in macroscopic structures that were no longer aligned in the flow direction.

Neither canola oil emulsions nor pectin-based MGP affected the formation of anisotropic structures within the investigated concentration range. Although slight changes in disulfide bond formation were observed with oil addition, the effect appeared too small to influence structure formation.

Overall, the results suggest that pH shifting can be used to modify structure formation during high-moisture extrusion, whereas oil and pectin-based MGP addition at the investigated concentrations was insufficient to induce structural changes. Future studies should investigate potential interactions between multiple additives, as these may provide further insight into structure formation mechanisms as well as the targeted formation of structures. The temperature sweep method furthermore proved effective in indicating changes in network formation and structure generation compared to the reference sample.

CRediT authorship contribution statement

Désirée Martin: Writing – original draft, Visualization, Validation, Supervision, Project administration, Methodology, Conceptualization. **Leon Harnisch:** Visualization, Validation, Investigation, Formal analysis. **Nico Leister:** Writing – review & editing, Supervision. **Ulrike S. van der Schaaf:** Writing – review & editing, Supervision, Resources. **Felix Ellwanger:** Writing – review & editing, Writing – original draft, Visualization, Validation, Supervision, Project administration, Methodology, Conceptualization.

Funding

The project was implemented without external funding.

Declaration of competing interest

The authors declare that they have no known competing financial interests or personal relationships that could have appeared to influence the work reported in this paper.

Acknowledgements

The authors would like to thank Herbstreith and Fox for providing the sugar beet pectin as well as Dyhydromatics LLC for providing the Shear Jet HL 60 and for their support. Many thanks to Kerstin Sauther, who patiently supported the extrusion trials.

Appendix A. Supplementary data

Supplementary data to this article can be found online at https://doi.org/10.1016/j.foodres.2026.120006.

Data availability

Data will be made available on request.

References

Akdogan, H. (1999). High moisture food extrusion. *International Journal of Food Science and Technology, 34*, 195. https://doi.org/10.1046/j.1365-2621.1999.00256.x

Arêas, J. A. (1992). Extrusion of food proteins. *Critical Reviews in Food Science and Nutrition, 32*, 365. https://doi.org/10.1080/10408399209527604

Baig, M. A., Ajayi, F. F., Hamdi, M., Baba, W., Brishti, F. H., Khalid, N., … Maqsood, S. (2025). Recent research advances in meat analogues: A comprehensive review on production, protein sources, quality attributes, analytical techniques used, and consumer perception. *Food Reviews International, 41*, 236–267. https://doi.org/10.1080/87559129.2024.2396855

Beniwal, A. S., Singh, J., Kaur, L., Hardacre, A., & Singh, H. (2021). Meat analogs: Protein restructuring during thermomechanical processing. *Comprehensive Reviews in Food Science and Food Safety, 20*, 1221–1249. https://doi.org/10.1111/1541-4337.12721

Cheftel, J. C., Kitagawa, M., & Quéguiner, C. (1992). New protein texturization processes by extrusion cooking at high moisture levels. *Food Review International, 8*, 235. https://doi.org/10.1080/87559129209540940

Chen, J., & Dickinson, E. (1999). Effect of surface character of filler particles on rheology of heat-set whey protein emulsion gels. *Colloids and Surfaces B: Biointerfaces, 12*, 373–381. https://doi.org/10.1016/S0927-7765(98)00091-5

Csapá, J., Csapó-Kiss, Z., Wágner, L., Tálos, T., Martin, T. G., Folestad, S., Tivesten, A., & Némethy, S. (1997). Hydrolysis of proteins performed at high temperatures and for short times with reduced racemization, in order to determine the enantiomers of d- and l-amino acids. *Analytica Chimica Acta, 339*, 99–107. https://doi.org/10.1016/S0003-2670(96)00452-7

Ebert, S., Gibis, M., Terjung, N., & Weiss, J. (2020). Survey of aqueous solubility, appearance, and pH of plant protein powders from carbohydrate and vegetable oil production. *LWT, 133*, Article 110078. https://doi.org/10.1016/j.lwt.2020.110078

Ellwanger, F., Fuhrmann, M., Karbstein, H. P., & Saavedra Isusi, G. I. (2024). Influence of lowering the pH value on the generation of fibrous structures of protein gels with different network types. *Gels, 10*, Article 173. https://doi.org/10.3390/gels10030173

Emin, M.A., Quevedo, M., Wilhelm, M., Karbstein, H.P., 2017. Analysis of the reaction behavior of highly concentrated plant proteins in extrusion-like conditions. Innovative Food Science & Emerging Technologies, Emerging Technologies with reference to IUFoST 44, 15–20. doi:https://doi.org/10.1016/j.ifset.2017.09.013.

Foegeding, E. A., Bowland, E. L., & Hardin, C. C. (1995). Factors that determine the fracture properties and microstructure of globular protein gels. *Food Hydrocolloids, 9*, 237–249. https://doi.org/10.1016/S0268-005X(09)80254-3

Gobes, M. I., Kuijpers, S. A., Terenzi, C., van der Sman, R. G. M., van Duynhoven, J. P. M., & Hohlbein, J. (2025). Rotated Fourier transform (RFT) enables the quantification of anisotropic structure in high-moisture plant-protein extrudates. *Food Structure, 44*, Article 100437. https://doi.org/10.1016/j.foostr.2025.100437

Gräfenhahn, M., & Beyrer, M. (2025). Influence of temperature and shear rate during cooling on the rheological and textural properties of pea protein-based meat analogues. *Journal of Food Engineering, 399*, Article 112625. https://doi.org/10.1016/j.jfoodeng.2025.112625

Grossmann, L., & McClements, D. J. (2023). Current insights into protein solubility: A review of its importance for alternative proteins. *Food Hydrocolloids, 137*, Article 108416. https://doi.org/10.1016/j.foodhyd.2022.108416

Harper, J. M. (2019). *Extrusion of foods*. Boca Raton: CRC Press. https://doi.org/10.1201/9780429290428

Kishore, D., Kundu, S., & Kayastha, A. M. (2012). Thermal, chemical and pH induced denaturation of a multimeric β-galactosidase reveals multiple unfolding pathways. *PLoS One, 7*. https://doi.org/10.1371/journal.pone.0050380

Koyama, S., Oka, D., Tsujii, Y., Takano, K., & Handa, A. (2020). Effects of lanthionine and Lysinoalanine on heat-induced gelation of egg white. *FSTR, 26*, 789–795. https://doi.org/10.3136/fstr.26.789

Kuijpers, S.A., Garina, E.D., Gobes, M.I., Adel, R. den, Smith, G.N., Sztucki, M., Hohlbein, J., Bouwman, W.G., van Duynhoven, J.P.M., Terenzi, C., 2025. Impact of pH-shifting on multiscale structural anisotropy of high-moisture extrudates of soy proteins. Food Hydrocolloids 168, 111456. doi:https://doi.org/10.1016/j.foodhyd.2025.111456.

Lagrain, B., De Vleeschouwer, K., Rombouts, I., Brijs, K., Hendrickx, M. E., & Delcour, J. A. (2010). The kinetics of β-elimination of cystine and the formation of lanthionine in gliadin |. *Journal of Agricultural and Food Chemistry, 58*, 10761–10767. https://doi.org/10.1021/jf102575r

Langstraat, T.D., Jansens, K.J.A., Delcour, J.A., Puyvelde, P.V., Goderis, B., 2015. Controlling wheat gluten cross-linking for high temperature processing. Industrial Crops and Products, Special issue derived from International Conference on Bio-based Materials and Composites 72, 119–124. doi:https://doi.org/10.1016/j.indcrop.2014.11.058.

Li, J., Janssen, F., Vallaey, A., Verfaillie, D., Brijs, K., Delcour, J. A., van der Goot, A. J., Van Royen, G., & Wouters, A. G. B. (2026). Understanding the effect of pH on structure formation in high moisture extrudates produced from soy protein-dietary fiber blends. *Food Hydrocolloids, 170*, Article 111710. https://doi.org/10.1016/j.foodhyd.2025.111710

Liu, R., Frederiksen, C. P., Rasmussen, T. R., Bakalis, S., Jensen, P. E., Rudić, S., … Gouseti, O. (2025). Effect of heat treatment on the molecular and functional properties of pea protein isolate. *Food Biophysics, 20*, 64. https://doi.org/10.1007/s11483-025-09954-x

Martin, D., Müller, E., & van der Schaaf, U. S. (2025). Formulation of high protein pea gels: Oil and microgel particles from pectin modulate the rheological, tribological and optical properties. *Food Hydrocolloids, 169*, Article 111595. https://doi.org/10.1016/j.foodhyd.2025.111595

McClements, D. J. (2024). Soft matter physics approaches for creating plant-based meat analogs. *Current Opinion in Food Science, 55*, Article 101120. https://doi.org/10.1016/j.cofs.2023.101120

Meißner, M. (2016). *Standard-Methoden für Getreide, Mehl und Brot mit allen aktuellen (ICC-Standards)*.

Monahan, F. J., German, J. B., & Kinsella, J. E. (1995). Effect of pH and temperature on protein unfolding and thiol/disulfide interchange reactions during heat-induced gelation of whey proteins. *Journal of Agricultural and Food Chemistry, 43*, 46–52. https://doi.org/10.1021/jf00049a010

Muhialdin, B. J., & Ubbink, J. (2023). Effects of pH and aging on the texture and physicochemical properties of extruded pea protein isolate. *Food Hydrocolloids, 140*, Article 108639. https://doi.org/10.1016/j.foodhyd.2023.108639

Muzammil, S., Kumar, Y., & Tayyab, S. (1999). Molten globule-like state of human serum albumin at low pH. *European Journal of Biochemistry, 266*, 26–32. https://doi.org/10.1046/j.1432-1327.1999.00810.x

Nieto-Nieto, T. V., Wang, Y. X., Ozimek, L., & Chen, L. (2015). Inulin at low concentrations significantly improves the gelling properties of oat protein – A molecular mechanism study. *Food Hydrocolloids, 50*, 116–127. https://doi.org/10.1016/j.foodhyd.2015.03.031

Nieuwland, M., Heijnis, W., van der Goot, A.-J., & Hamoen, R. (2023). XRT for visualizing microstructure of extruded meat replacers. *Current Research in Food Science, 6*, Article 100457. https://doi.org/10.1016/j.crfs.2023.100457

Nisov, A., Nikinmaa, M., Nordlund, E., & Sozer, N. (2022). Effect of pH and temperature on fibrous structure formation of plant proteins during high-moisture extrusion processing. *Food Research International, 156*, Article 111089. https://doi.org/10.1016/j.foodres.2022.111089

Opaluwa, C., Deskovski, S., Karbstein, H. P., & Emin, M. A. (2024). Effect of oil on the rheological properties and reaction behavior of highly concentrated wheat gluten under conditions relevant to high moisture extrusion. *Future Foods, 9*, Article 100307. https://doi.org/10.1016/j.fufo.2024.100307

Pernice, L., Röhrich, D., Gaukel, V., & Leister, N. (2025). Enhancing variability in fibrous structures via geometric modifications of breaker plates in high-moisture extrusion of meat analogues. *Journal of Food Engineering, 399*, Article 112602. https://doi.org/10.1016/j.jfoodeng.2025.112602

Pietsch, V. L., Emin, M. A., & Schuchmann, H. P. (2017). Process conditions influencing wheat gluten polymerization during high moisture extrusion of meat analog products. *Journal of Food Engineering, 198*, 28–35. https://doi.org/10.1016/j.jfoodeng.2016.10.027

Saavedra I., G.I., Pietsch, V., Beutler, P., Hoehne, S., Leister, N., 2023. Influence of rapeseed oil on extruded plant-based meat analogues: Assessing mechanical and rheological properties. Processes 11, 1871. doi:https://doi.org/10.3390/pr11071871.

Saavedra Isusi, G. I., Lohner, N., Karbstein, H. P., & van der Schaaf, U. S. (2021). Emulsions stabilised with pectin-based microgels: Investigations into the break-up of droplets in the presence of microgels. *Journal of Food Engineering, 294*, Article 110421. https://doi.org/10.1016/j.jfoodeng.2020.110421

Scheraga, H. A., Némethy, G., & Steinberg, I. Z. (1962). The contribution of hydrophobic bonds to the thermal stability of protein conformations. *Journal of Biological Chemistry, 237*, 2506–2508. https://doi.org/10.1016/S0021-9258(19)73780-6

Schmid, E.-M., Farahnaky, A., Adhikari, B., & Torley, P. J. (2022). High moisture extrusion cooking of meat analogs: A review of mechanisms of protein texturization. *Comprehensive Reviews in Food Science and Food Safety, 21*, 4573–4609. https://doi.org/10.1111/1541-4337.13030

Schumacher, T., Steinmacher, T., Köster, E., Wagemans, A., Weiss, J., & Gibis, M. (2025). Physico-chemical characterization of ten commercial pea protein isolates. *Food Hydrocolloids, 162*, Article 110996. https://doi.org/10.1016/j.foodhyd.2024.110996

Schwass, D. E., & Finley, J. W. (1984). Heat and alkaline damage to proteins: Racemization and lysinoalanine formation. *Journal of Agricultural and Food Chemistry, 32*, 1377–1382. https://doi.org/10.1021/jf00126a040

van der Sman, R. G. M., & van der Goot, A. J. (2023). Hypotheses concerning structuring of extruded meat analogs. *Current Research in Food Science, 6*, Article 100510. https://doi.org/10.1016/j.crfs.2023.100510

Tokmakov, A. A., Kurotani, A., & Sato, K.-I. (2021). Protein pI and intracellular localization. *Frontiers in Molecular Biosciences, 8*. https://doi.org/10.3389/fmolb.2021.775736

Totasaus, A., Montejano, J. G., Salazar, J. A., & Guerrero, I. (2002). Review of physical and chemical protein-gel induction | International journal of food science and technology | Oxford academic. *International Journal of Food Science & Technology, 37*, 589–601. https://doi.org/10.1046/j.1365-2621.2002.00623.x

Totosaus, A., Montejano, J. G., Salazar, J. A., & Guerrero, I. (2002). A review of physical and chemical protein-gel induction. *International Journal of Food Science and Technology, 37*, 589. https://doi.org/10.1046/j.1365-2621.2002.00623.x

Wittek, P., Ellwanger, F., Karbstein, H. P., & Emin, M. A. (2021). Morphology development and flow characteristics during high moisture extrusion of a plant-based meat analogue. *Foods, 10*, 1753. https://doi.org/10.3390/foods10081753

Wittek, P., Zeiler, N., Karbstein, H. P., & Emin, M. A. (2020). Analysis of the complex rheological properties of highly concentrated proteins with a closed cavity rheometer. *Applied Rheology, 30*, 64–76. https://doi.org/10.1515/arh-2020-0107

Wu, S., Liu, Y., Song, H., Jiang, L., Yan, S., & Qi, B. (2025). Formation of cross-linked lysinoalanine in soy protein isolate: Synergy between hot-alkali and pH-shift treatments. *International Journal of Biological Macromolecules, 308*, Article 142614. https://doi.org/10.1016/j.ijbiomac.2025.142614